Journal Pre-proof

Simple analogues of natural product chelerythrine: Discovery of a novel anticholinesterase 2-phenylisoquinolin-2-ium scaffold with excellent potency against acetylcholinesterase

Bohang Zhou, Hui Li, Zhiming Cui, Ding Li, Huiling Geng, Jinming Gao, Le Zhou

PII: S0223-5234(20)30386-X

DOI: https://doi.org/10.1016/j.ejmech.2020.112415

Reference: EJMECH 112415

To appear in: *European Journal of Medicinal Chemistry*

Received Date: 1 March 2020

Revised Date: 16 April 2020

Accepted Date: 29 April 2020

Please cite this article as: B. Zhou, H. Li, Z. Cui, D. Li, H. Geng, J. Gao, L. Zhou, Simple analogues of natural product chelerythrine: Discovery of a novel anticholinesterase 2-phenylisoquinolin-2-ium scaffold with excellent potency against acetylcholinesterase, *European Journal of Medicinal Chemistry* (2020), doi: https://doi.org/10.1016/j.ejmech.2020.112415.

This is a PDF file of an article that has undergone enhancements after acceptance, such as the addition of a cover page and metadata, and formatting for readability, but it is not yet the definitive version of record. This version will undergo additional copyediting, typesetting and review before it is published in its final form, but we are providing this version to give early visibility of the article. Please note that, during the production process, errors may be discovered which could affect the content, and all legal disclaimers that apply to the journal pertain.

© 2020 Published by Elsevier Masson SAS.

Graphical Abstract

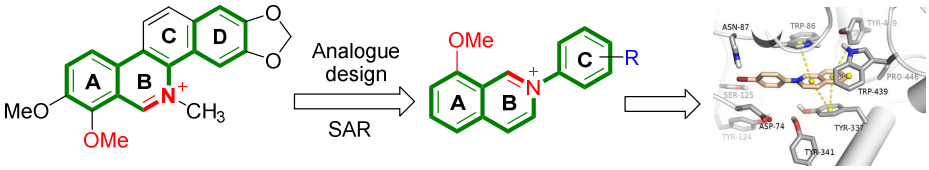

Chelerythrine
IC_{50} = 1.45 μM, AChE;
8.54 μM, BuChE

Target compounds (8)
7 compounds:
$IC_{50} \leq 0.72$ μM, AChE

8y: IC_{50} = 0.14 μM, AChE;
3.84 μM, BuChE
Cytotoxicity: $IC_{50} > 50$ μM

Journal Pre-proof

Journal Pre-proof

Full paper

Simple Analogues of Natural Product Chelerythrine: Discovery of a Novel Anticholinesterase 2-Phenylisoquinolin-2-ium Scaffold with Excellent Potency against Acetylcholinesterase

Bohang Zhou[§], Hui Li[§], Zhiming Cui, Ding Li, Huiling Geng,* Jinming Gao,* and Le Zhou*

College of Chemistry & Pharmacy, Northwest A&F University, 22 Xinong Road, Yangling, 712100, Shaanxi, China

*Corresponding author. *E-mail address*: zhoulechem@nwsuaf.edu.cn (L. Zhou); jinminggao@nwafu.edu.cn (J. Gao); genghuiling5@163.com (H. Geng)

[§] These authors contributed equally to this work.

Journal Pre-proof

Journal Pre-proof

ABSTRACT

As simple analogues of the natural compound chelerythrine, a novel anti-cholinesterase 2-phenylisoquinolin-2-ium scaffold was designed by structure imitation. The activity evaluation led to the discovery of seven compounds with potent anti-acetylcholinesterase activity with IC_{50} values of ≤ 0.72 μM, superior to chelerythrine and standard drugs galantamine. Particularly, compound **8y** showed the excellent dual acetylcholinesterase-butyrylcholinesterase inhibition activity, superior to rivastigmine, a dual cholinesterase inhibitor drug. Furthermore, the compounds displayed a competitive anti-acetylcholinesterase mechanism with the substrate and low cytotoxicity. Molecular docking showed that the isoquinoline moiety is embedded in a cavity surrounded by four aromatic residues of acetylcholinesterase by the π-π action. Structure-activity relationship showed that the *p*-substituents on the C-ring can dramatically improve the anti-acetylcholinesterase activity, while 8-OMe can increase the activity against the two cholinesterases simultaneously. Thus, the title compounds emerged as promising lead compounds for the development of novel cholinesterase inhibitor agents.

Keywords:

Isoquinoline

Benzo[*c*]phenanthridine

Acetylcholinesterase

Butyrylcholinesterase

Structure-activity relationship

Molecular docking

Journal Pre-proof

Journal Pre-proof

1. Introduction

Cholinesterases (ChE) include two types of enzymes, namely acetylcholinesterase (AChE) and butyrylcholinesterase (BuChE). The most striking difference between them is that AChE preferentially hydrolyzes acetylcholine (ACh) while BuChE hydrolyzes butyrylcholine (BuCh) more efficiently than ACh. Furthermore, histologically, AChE is mostly of neuronal origin, while BuChE is primarily present in the blood and glial cells [1].

ACh is one type of ubiquitous neurotransmitter. The main function of AChE is to modulate cholinergic signal transmission through hydrolysis of ACh. Under normal conditions, ACh is dominantly decomposed by AChE instead of BuChE [2]. However, when the level of AChE in cholinergic transmission declines, BuChE can play a function compensation role for AChE to some extent to maintain normal cholinergic pathways [3]. Therefore, ChE inhibitors are very interesting candidates for development of medicines for treatment of some neurogenic diseases related with cholinergic transmission, such as Alzheimer's disease (AD), senile dementia, ataxia and myasthenia gravis [4]. Additionally, AChE inhibitors can also be used for development of insecticides [5].

AD is one of the most common, age-related irreversible and progressive neurodegenerative disorders characterized as dementia, memory loss, a decline in language skills and cognitive impairment with aging [6]. The number of people with AD will be expected to reach over 131 million by 2050 [7]. Therefore, AD has been one of the main public health issues we have to face.

The pathogenesis of AD involves different molecular events such as low level of acetylcholine (ACh) [8], β-amyloid (Aβ) aggregation [9], tau-protein hyperphosphorylation [10] and oxidative stress [11], etc. Among them, low level of ACh in different areas of the central nervous system has been proved to be associated with the memory impairment and behavioral abnormalities in patients with AD [12]. Based on the results above, some AChE inhibitor (AChEI) agents have been developed and used for treatment of cognitive dysfunction and memory loss of mild-to-moderate AD patients by elevating the level of ACh in brain, such as tacrine, donepezil, galantamine, rivastigmine, etc [13,14]. However, except for rivastigmine, a dual AChE−BuChE inhibitor, these selective AChE inhibitor drugs are not suitable for the late stage AD since ACh hydrolysis in the late stage of AD mainly depends on BuChE but not AChE [3]. Furthermore, some obvious adverse effects like nausea and vomiting, decreased appetite, weight loss, hepatotoxicity, etc. were also reported for these drugs [15]. Therefore, the search of more ideal ChE inhibitors (ChEIs), especially dual AChE−BuChE inhibitors is very necessary for treatment of AD [16].

Sanguinarine (SA) and chelerythrine (CH) (Fig. 1), two most common quaternary benzo[*c*]phenanthridine alkaloids (QBAs), can be considered as ideal leading compounds for development of novel ChEIs based on their good dual AChE−BuChE inhibition [17], excellent cellular permeability [18] and high safety for mammal [19]. This study aims to search for QBA-like cholinesterase inhibitors (ChEIs) with more simple structure and more potent activity than SA or CH.

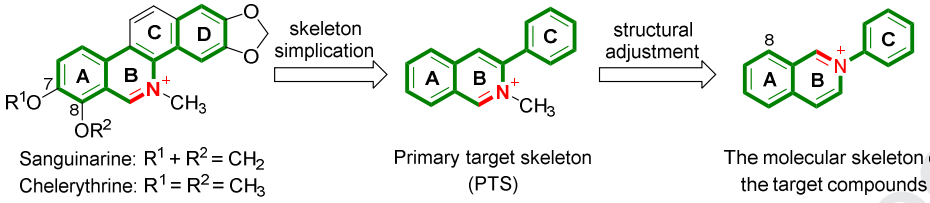

Figure 1. Design of the basic skeleton of the target compounds by structure imitation.

In the present study, as structurally simple analogues of QBAs, a class of novel 2-arylisoquinolin-2-ium salts were designed by structure imitation, synthesized and evaluated for AChE and BuChE inhibition activities in vitro. Furthermore, the kinetic action mechanism, molecular docking, structure-activity relationship (SAR) and cytotoxicity were also investigated. To our knowledge, no reports have been found on the anti-ChE activity of 2-arylisoquinolin-2-ium compounds until now.

2. Results and discussion

2.1. Rational design of target compounds

The most remarkable structural feature of SA and CH (Fig. 1) is the presence of one benzo[*c*]phenanthridine framework and a highly polar iminium moiety (C=N$^+$). Our previous study proved that the iminium moiety is a determinant for the bioactivities of SA and CH, including anticancer [20], acaricidal [21] and antimicrobial [22, 23]. A similar case was also found in the anti-AChE and antifungal activities of their analogues 2-aryl-β-carbolin-2-iums and their 3,4-dihydro derivatives [24, 25]. Therefore, we speculated that a similar case may well also exist in ChE inhibition activity of SA and CH.

Based on the findings above and the principle of analogue design, we initially designed one primary target skeleton (PTS) (Fig. 1) by deleting the C-ring of SA or CH, which is considered as a simplified QBAs-like skeleton. Next, considering that SA or CH can be metabolized to the corresponding neutral nonactive phenanthridine derivative by demethylation (N-Me) in cells [26], we further adjusted and simplified the structure of PTS by

deleting the (N-)methyl and changing the position of the nitrogen atom to obtain the present target molecule framework (Fig. 1). Obviously, the framework of the target molecules possesses the similar molecular length, width and polar iminium moiety (C=N$^+$) as SA or CH. Therefore, theoretically, the target compounds should also have ChE inhibition activity like SA or CH.

In aspects of substituents, almost all of the known QBAs have one alkoxy group at 7 site adjacent to its C=N$^+$ bond. According to this characteristic, we further designed an 8-methoxy on the target skeleton to obtain the parent compound, i.e., 2-phenyl-8-methoxyisoquinolin-2-ium (**8a**, Fig. 2). Meanwhile, compound **8zf** without 8-OMe was also designed to examine the effect of 8-OMe on the activity.

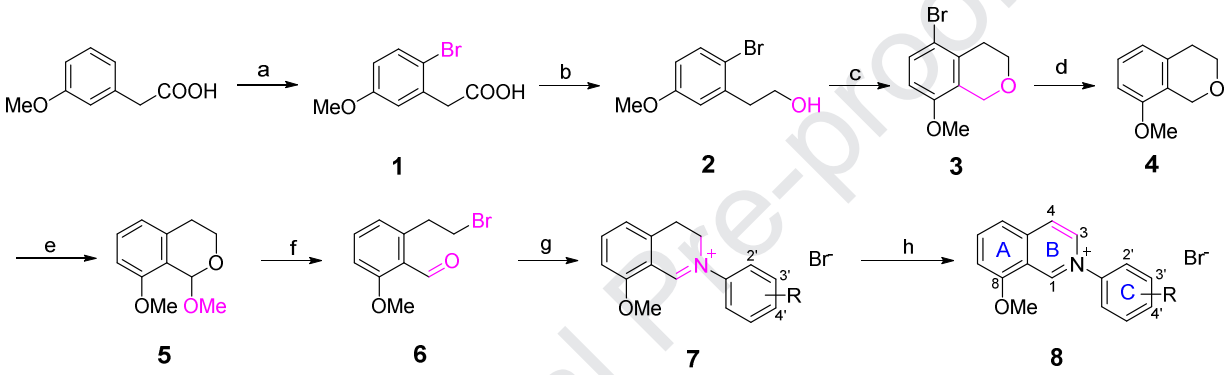

	R		R		R
8a / 7a	H	**8l / 7l**	3'-I	**8w / 7w**	2'-OMe
8b / 7b	2'-F	**8m / 7m**	4'-I	**8x / 7x**	3'-OMe
8c / 7c	3'-F	**8n / 7n**	2'-CF_3	**8y / 7y**	4'-OMe
8d / 7d	4'-F	**8o / 7o**	3'-CF_3	**8z / 7z**	2',6'-2F
8e / 7e	2'-Cl	**8p / 7p**	4'-CF_3	**8za / 7za**	2',4'-2Cl
8f / 7f	3'-Cl	**8q / 7q**	2'-CN	**8zb / 7zb**	3',5'-2Cl
8g / 7g	4'-Cl	**8r / 7r**	3'-CN	**8zc / 7zc**	2',4'-2Br
8h / 7h	2'-Br	**8s / 7s**	4'-CN	**8zd / 7zd**	2'-F-4'-Br
8i / 7i	3'-Br	**8t / 7t**	2'-Me	**8ze / 7ze**	2'-F-4'-I
8j / 7j	4'-Br	**8u / 7u**	3'-Me		
8k / 7k	2'-I	**8v / 7v**	4'-Me		

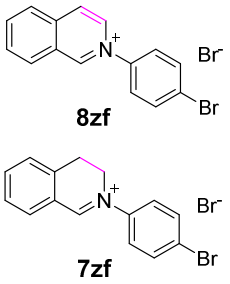

Figure 2. Synthesis route of the target compounds **(8)**. (a) Br_2, dry DCM; (b) $NaBH_4$, I_2, dry THF, 40 °C; (c) $(HCHO)_n$, TFA, 0 °C to rt; (d) *n*-BuLi, dry THF, –78 °C, and then treated with water; (e) DDQ, dry MeOH, dry DCM; (f) TMSBr, Bu_4NBr, dry toluene, 80 °C; (g) Ar-NH_2, dioxane ;(h) Pd/C, acetonitrile, reflux.

Electron density distribution and stereochemistry are two important impact factors for the bioactivity of molecules. Theoretically, the substituents on the C-ring not only can influence the electron density distribution of the target molecules but also its stereochemistry such as the dihedral angle between the B-ring and C-ring. With the aim of finding more potent AChE inhibitors and understanding the structure-activity relationship, various substitution patterns were designed on the C-ring (Table 1). The substituents include

Journal Pre-proof

electron withdrawing groups like halogen atoms, trifluoromethyl and cyano and electron-donating groups like methyl and methoxy. The substitution sites involve ortho-, meta- and para-position (Fig. 2).

2.2. Synthesis of compounds

The synthetic route is shown in Figure 2. According to our reported method [27], intermediates **7** were synthesized from commercially available 2-(3-methoxyphenyl) acetic acid as a starting material *via* bromination, reduction of carboxyl group, cyclization with paraformaldehyde in trifluoroacetic acid, debromination with *n*-BuLi, oxidation with DDQ in the presence of methanol, ring-opening with Bu_4NBr in the presence of TMSBr and finally reaction with aniline or substituted anilines. **7zf** without 8-OMe was synthesized from 2-phenylethanol according to the method described in literature [28]. Compounds **7** were dehydrogenated by Pd/C in acetonitrile or toluene to provide the corresponding target compounds **8**.

Compounds **8** were structurally elucidated by ^1H NMR, ^{13}C NMR and HRMS analyses. The structures of intermediates **7** were confirmed by comparison of spectral data those reported in literature [27]. All compounds **8** showed some similar spectroscopic characteristics due to the structural similarity. Each compound showed a characteristic ion peak at *m*/*z* $[M-Br]^+$ in positive HRMS spectra. The presence of bromide anion was confirmed by ion peaks at *m*/*z* 79 and 81 in negative ESI-MS spectra. In ^1H and ^{13}C NMR spectra, each compound **8** revealed signals of H-1 at δ_H ca. 10.0 (1 H, s or d, J = ca. 1.2 Hz) and C-1 in the range of δ_C 158–160, signals of one AX system at δ_H ca. 8.88 (1 H, d, J = ca 6.5 Hz, H-4), ca. 8.56 (1 H, d, J = ca. 6.5 Hz, H-3), δ_C ca. 146 (C-4) and ca.140 (C-3). Except **8zf**, all compounds **8** also showed signals of 8-OMe in the range of δ_H 3.0–4.3 and δ_C ca. 56.5.

2.3. ChE inhibition activity

According to Ellman's method [29], compounds **8** along with intermediates **7** were initially screened for inhibition activity on AChE at 10 μM. SA and CH as model compounds were used as reference controls. Galantamine, a selective AChE inhibitor drug for treatment of AD, was used as a positive control.

As expected, all compounds **8** showed anti-AChE activity at 10 μM in varying degrees like SA or CH (Figure 3). A similar case was also found for **7**. However, **8** were obviously more active than the respective **7**

in most cases. It is worth noting that some compounds (**8g**, **8j**, **8p**, **8y**, **8zc**, **8zd**, **7g**, **7j**) displayed the excellent activity with inhibition rates of >90%, comparable with galantamine.

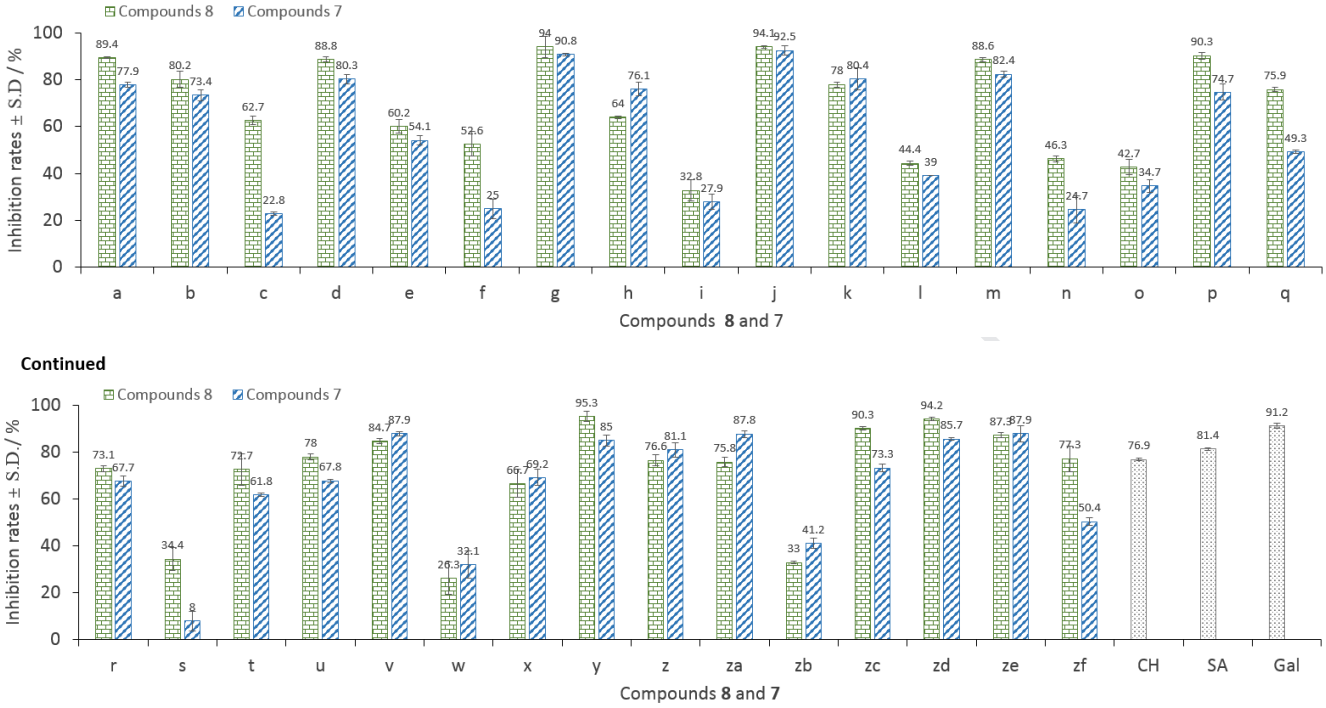

Figure 3. The activity of compounds **8** and **7** against AChE at 10 μM. CH: chelerythrine; SA: sanguinarine; Gal: galantamine.

In order to explore anti-AChE potential in more detail, selectivity to both AChE and BuChE as well as SAR, the more active compounds with the inhibition rates of ＞50% in Figure 3 were further determined for median inhibition concentrations (IC_{50}) on both AChE and BuChE. The results are shown in Table 1.

Gratifyingly, seven out of **8** (**8d**, **8g**, **8j**, **8m**, **8p**, **8y**, **8zc**) gave lower IC_{50} values of 0.14 to 0.72 μM for AChE than galantamine (IC_{50} 0.79 μM) and SA and CH (IC_{50} 1.22, 1.45 μM). A similar case was also observed for three **7** (**7h**, **7j**, **7v**). Among them, **8g**, **8j** and **8y** gave the highest anti-AChE activity (IC_{50} 0.1–0.2 μM), which reached up to more than four-fold that of galantamine. The results above strongly supported the rationality of our target molecular design idea. Furthermore, most of the tested compounds also showed some anti-BuChE activity (IC_{50} > 20 μM), but which is much less active than the respective anti-AChE activity and that of SA and CH (IC_{50} 7.08, 8.58 μM). Obviously, this kind of compounds has higher selectivity to AChE relative to BuChE. It was worth noting that **8y** revealed the excellent inhibition activities on both AChE and BuChE (IC_{50} 0.14, 3.84 μM) simultaneously, comparable with rivastigmine (IC_{50} 9.94, 2.86 μM), a dual

AChE−BuChE inhibitor drug. Therefore, **8y** can be considered as one promising candidate compound for development of novel dual AChE−BuChE inhibitor drug.

Table 1
Median inhibition concentrations of compounds **8** and intermediates **7** against ChEs.

No.	IC_{50} (95%CI) (μM)		SI[a]	No.	IC_{50} (95%CI) (μM)		SI[a]
	AChE	BuChE			AChE	BuChE	
8a	1.42 (1.23–1.62)	80.3 (75.9–84.9)	56.5	**7a**	1.62 (1.40–1.84)	35.4 (30.0–42.6)	21.9
8b	2.55 (2.11–3.10)	80.9 (73.1–88.9)	31.7	**7b**	2.94 (2.68–3.22)	75.0 (66.7–83.6)	25.5
8c	9.13 (7.44–11.9)	>250		**7c**	>10[b]	n.d.[c]	
8d	**0.67** (0.41–0.75)	143 (126–166)	213	**7d**	1.99 (1.80–2.17)	113 (94.2–133)	56.8
8e	5.33 (4.84–5.94)	67.2 (56.4–77.6)	12.6	**7e**	≈10[b]	190 (172–211)	19.0
8f	9.45 (7.66–12.3)	36.4 (29.4–44.3)	3.85	**7f**	>10[b]	n.d.[c]	
8g	**0.17** (0.12–0.23)	105 (97.9–114)	618	**7g**	**0.32** (0.25–0.38)	62.1 (57.8–67.0)	194
8h	5.23 (4.83–5.69)	89.5 (80.7–98.9)	17.1	**7h**	1.50 (1.15–1.83)	27.2 (21.8–33.1)	18.1
8i	>10[b]	n.d.[c]		**7i**	>10[b]	n.d.[c]	
8j	**0.19** (0.13–0.26)	21.6 (17.7–25.6)	114	**7j**	**0.28** (0.22–0.34)	20.7 (17.2–24.4)	73.9
8k	2.06 (1.84–2.27)	36.9 (34.7–39.2)	17.9	**7k**	1.79 (1.58–2.00)	28.9 (26.1–31.8)	16.1
8l	>10[b]	n.d.[c]		**7l**	>10[b]	n.d.[c]	
8m	**0.72** (0.53–0.91)	36.1 (32.6–39.6)	50.1	**7m**	1.01 (0.76–1.24)	58.1 (43.7–71.3)	57.5
8n	>10[b]	n.d.[c]		**7n**	>10[b]	n.d.[c]	
8o	>10[b]	n.d.[c]		**7o**	>10[b]	n.d.[c]	
8p	**0.69** (0.62–0.77)	33.5 (26.4–41.7)	48.6	**7p**	1.94 (1.56–2.30)	221 (193–256)	114
8q	1.75 (1.52–1.94)	59.4 (55.7–63.4)	33.9	**7q**	≈10[b]	n.d.[c]	
8r	3.41 (3.22–3.62)	>250		**7r**	5.31 (4.73–5.97)	110 (103–119)	20.7
8s	>10[b]	n.d.[c]		**7s**	>10[b]	n.d.[c]	
8t	2.89 (2.55–3.23)	243 (224–265)	37.8	**7t**	3.07 (2.62–3.43)	133 (107–165)	
8u	2.21 (1.75–2.50)	30.6 (27.8–33.4)	13.8	**7u**	2.89 (2.25–3.53)	35.9 (32.4–39.4)	8.8
8v	1.08 (0.94–1.24)	>250		**7v**	**0.53** (0.42–0.64)	47.1 (42.1–52.4)	
8w	>10[b]	n.d.[c]		**7w**	>10[b]	n.d.[c]	
8x	6.90 (6.27–7.62)	98.3 (85.5–111)	14.2	**7x**	5.23 (3.07–6.05)	77.3 (63.8–91.4)	14.8
8y	**0.14** (0.11–0.17)	**3.84** (3.17–4.54)	27.4	**7y**	1.04 (0.72–136)	113 (93.5–135)	128
8z	2.70 (2.45–2.96)	48.4 (43.1–53.6)	17.9	**7z**	1.29 (1.01–1.62)	105 (92.3–120)	81.4
8za	3.42 (3.02–3.93)	232 (213–256)	67.8	**7za**	1.04 (0.86–1.23)	90.5 (80.4–101)	87.0
8zb	>10[b]	n.d.[c]		**7zb**	>10[b]	n.d.[c]	
8zc	**0.57** (0.44–0.51)	131 (122–139)	230	**7zc**	3.72 (3.55–3.90)	116 (102–133)	31.2
8zd	**0.90** (0.82–0.98)	196 (176–223)	218	**7zd**	1.29 (1.03–1.54)	69.3 (63.7–74.8)	53.7
8ze	1.23 (1.05–1.45)	89.8 (81.7–98.4)	73.0	**7ze**	1.06 (0.87–1.36)	128 (107–153)	121
8zf	2.39 (2.18–2.62)	130 (115–146)	54.4	**7zf**	10.5 (9.38–11.9)	63.7 (55.1–73.8)	6.07
Sanguinarine	1.22 (1.10–1.34)	7.08 (4.27–10.2)	5.80	Rivastigmine	9.94 ± 0.83[d]	2.86 ± 0.22[d]	0.29[d]
Chelerythrine	1.45 (1.22–1.71)	8.58 (5.34–12.1)	5.92	Tacrine	0.25 ± 0.01[e]	0.05 ± 0.00[e]	0.22[e]
Galantamine	0.79 ± 0.05	13.7 ± 0.71	18.0	Donepezil	0.03 ± 0.01[f]	5.40 ± 0.27[f]	180[f]

[a] Selectivity index = the ratio value of IC_{50} (BuChE)/IC_{50} (AChE). [b] Estimated values based on the results in Figure 3. [c] n.d.: no determination. [d] The data are cited from ref. [30]. [e] The data are cited from ref. [31]. [f] The data are cited from ref. [32].

2.4. Cytotoxicity

In order to get insight into the toxicity of compounds **8** and **7**, three more active compounds **8j, 8y** and **8zc** along with their respective intermediates **7** were further evaluated for cytotoxic activity on three strains of

Journal Pre-proof

normal cells, mouse neuroblastoma N2a cells, primary cultured porcine fetal kidney cells and primary cultured goat fetal fibroblast using the 3-(4,5-dimethyl-2-thiazolyl)-2,5-diphenyl-2-H-tetrazolium bromide (MTT) method [20]. Compounds **8j** and **8y** were chosen as the representative compounds with an electron-withdrawing group and an electron-donating group, respectively, while **8zc** was chosen as the representative dihalogenated compound.

The results in Table 2 showed that both **8j, 8y** and **8zc**, especially the last two showed the much lower cytotoxicity (IC_{50} values > 19 μM) on all the tested cells than their anti-AChE activity (IC_{50} < 0.60 μM). A similar case was also observed for **7j, 7y** and **7zc** (IC_{50} 4.26–27.3 μM *vs* 0.28, 1.04, 3.72 μM). Relatively, the cytotoxicities of **8y** with 4′-OMe and **8zc** with 2′,4′-diBr were lower than **8j** with 4′-Br. However, compared with the corresponding intermediates **7**, compounds **8**, especially **8y** and **8zc** (IC_{50} > 50 μM) showed lower cytotoxicity on all the tested cells. The results above indicate that both aromatization of the B-ring and the presence of 4′-OMe are beneficial for low cytotoxicity of **8**. Thus, compounds **8** possess greater potential than **7** for development of new AChE inhibitor drugs in two aspects of anti-AChE activity and cytotoxicity.

Table 2

Cytotoxicity of the compounds on three strains of normal cells (48 h).

Compd.		IC_{50} (μM) (95% confidence interval)		
No.	R	Mouse neuroblastoma N2a cells	Primary cultured porcine fetal kidney cells	Primary cultured goat fetal fibroblast
8j	4′-Br	20.8 (15.9–27.2)	19.8 (15.8–27.0)	>50
8y	4′-OMe	>50	>50	>50
8zc	2′,4′-diBr	>50	>50	>50
7j	4′-Br	20.3 (17.0–24.2)	19.2 (16.1–23.0)	20.6 (14.4–29.5)
7y	4′-OMe	26.6 (21.3–30.1)	23.8 (18.4–27.5)	27.3 (23.5–32.9)
7zc	2′,4′-diBr	4.26 (4.09–4.44)	6.03 (5.60–6.48)	6.13 (5.22–7.20)

2.5. Mechanism of AChE inhibition

As representative compounds, **8j** and **7j** were conducted for kinetic analysis of AChE inhibition to explore the inhibition mechanism. The graphical analysis of the inhibition data is shown in Figure 4. Figures 4A and 4C clearly showed that the two compounds inhibited AChE in a competitive manner with the substrate acetylthiocholine iodide (ATCh). The inhibition constants K_i of **8j** and **7j** for AChE were 1.48×10^{-8} M and 8.86×10^{-8} M, respectively, indicating **8j** has approximately 6-fold the binding capacity of **7j** with AChE. Compared with the K_m value of 1.69×10^{-4} M of substrate ATCh, the binding capacity of **8j** with AChE reaches up to 11419-fold that of ATCh.

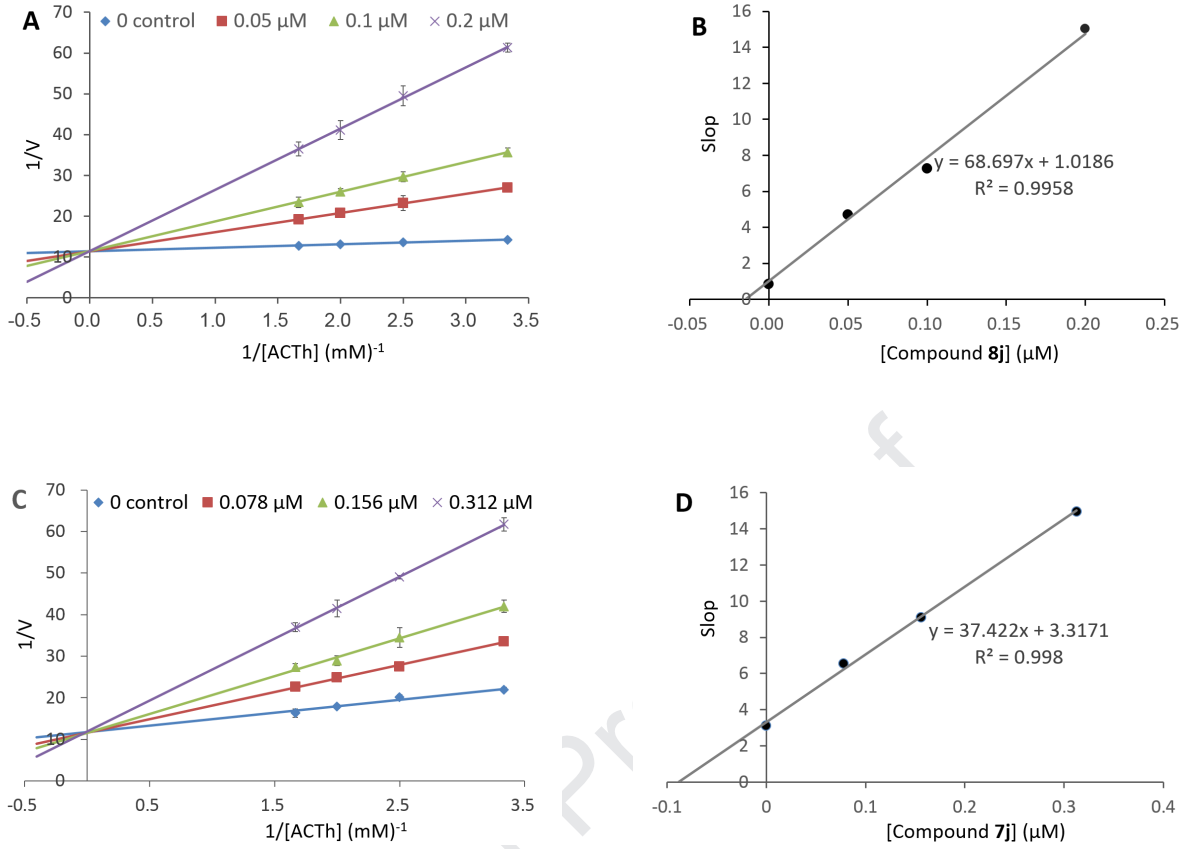

Figure 4. Mechanism of AChE inhibition by compound **8j** (**A**) and intermediate **7j** (**C**) respective to ATCh, and their K_i determination (**B, D**). **A** and **C**: the reciprocals of the initial reaction rates and substrate concentrations are plotted; **B** and **D**: the slope values of the lines from graph **A** or **C** are plotted versus the inhibitor concentrations, affording an equation of linear regression. When *y* is 0, the equations give *K*i values of 1.48×10^{-8} M for **8j** and 8.86×10^{-8} M for **7j**.

2.6. Molecular docking study

As representative compounds, compounds **8** with high anti-AChE activity were conducted for molecular docking studies to get insight into their binding interactions in the hydrolytic active site of AChE and BuChE. The data in Table 3 show that the binding free energies (FBE) of each the compound except **8d** with the catalytic site of AChE are larger than their respective FBE with BuChE, indicating that compounds **8** have more inhibition potential to AChE than BuChE, agreement with the measured inhibition activities. Additionally, there was an acceptable correlation between the FBE values and the pIC_{50} values ($P < 0.3059$) for AChE (see supporting information). However, no correlation was found for BuChE, which might be related with the lower anti-BuChE activity of the compounds and the larger measurement deviation of IC_{50} values.

Table 3

Estimated free energy of binding (FBE, kcal/mol) of the test compounds to the active cavities of AChE (PDB code: 4BDT) and BuChE (PDB code: 5K5E).

Compound	FBE (kcal/mol)		IC_{50} (μM)	
	AChE	BuChE	AChE	BuChE
8d	−6.16	−7.05	0.67	143
8g	−8.35	−7.54	0.17	105
8j	−7.69	−6.63	0.19	21.6
8m	−7.32	−6.57	0.72	36.1
8p	−7.05	−6.63	0.69	33.5
8v	−7.45	−6.53	1.08	>250
8y	−7.66	−6.49	0.14	3.84
8zc	−7.86	−7.07	0.57	131
huprine W[a]	−10.23	/	0.0011	
6QS[b]	/	−11.49		0.443

[a] The inhibitor co-crystals with AChE in the crystal structure of the protein complex (PDB code: 4BDT). [b] The inhibitor co-crystals with BuChE in the crystal structure of the protein complex (PDB code: 5K5E).

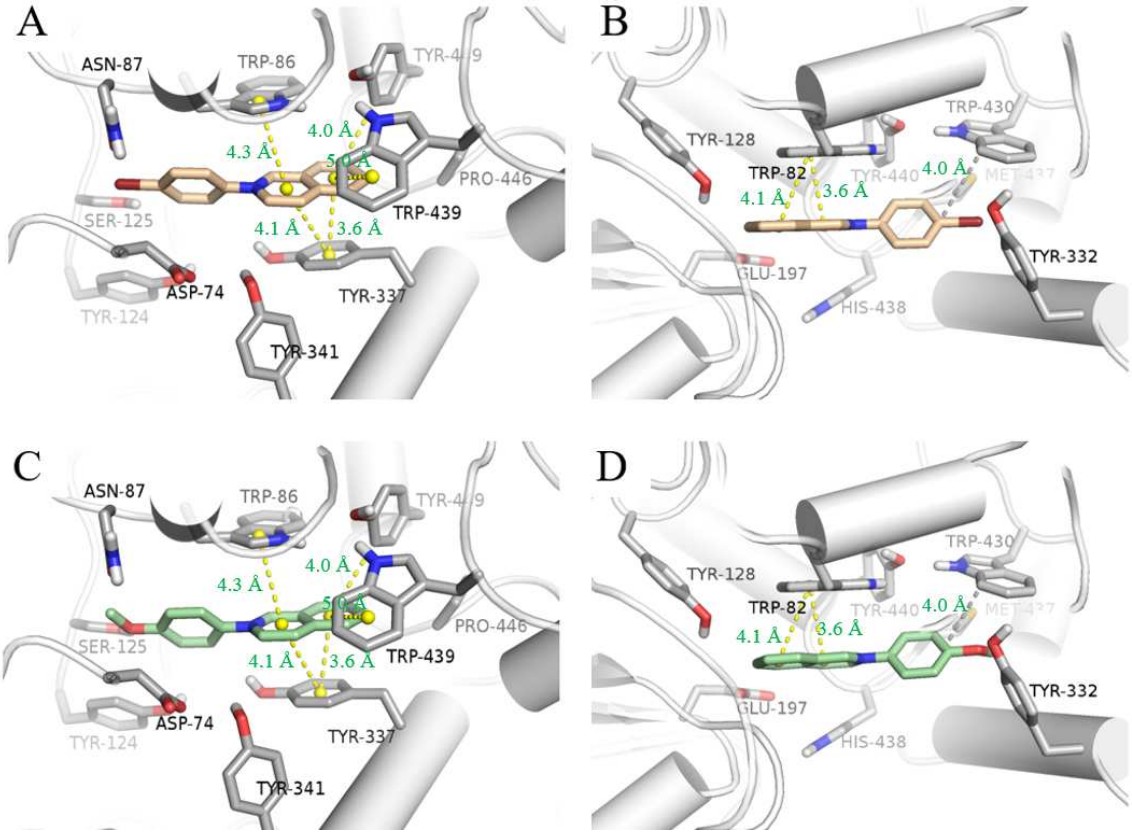

Journal Pre-proof

Figure 5. The estimated binding modes of the compounds (**8j**, in stick model with carbon in wheat; **8y**, in stick model with carbon in pale green) into the active site of AChE (A, C) and BuChE (B, D).

The results of molecular docking showed that **8j** and **8y** have very similar binding modes (Figure 5). Figure 5A and 5C showed that the isoquinoline moiety of the compounds is embedded in a remarkable group of aromatic rings including Trp86, Tyr337, Trp439 and Tyr449 by the π-π interactions between the A-, B-ring of the isoquinoline and the phenyl ring of Tyr337 (distance < 4.1 Å), the B-ring and the indole ring of Trp86 (distance = 4.3 Å), and the A-ring and the phenyl ring of Trp439 (distance = 5.0 Å). The results above indicated that the binding region of the AChE with the compounds **8** was the cationic site (Trp86) in the gorge of the AChE. Interestingly, the binding mode is very similar to that of 2-aryl-β-carbolin-2-iums.[25] It was worth noting that the positively charged isoquinoline moiety is poor in π-electron, whereas all the aromatic rings of these residues are rich in π-electrons. Therefore, the compounds can form strong π-π action with the residues to improve the overall affinity of AChE for the compounds or the activity of the compounds. Obviously, the aromatic B-ring in **8** can give stronger π-π action than the non-aromatic B-ring in **7**, which explains why compounds **8** have larger binding free energy with AChE (Table 3) and higher anti-AChE activity than the corresponding **7** (Table 1).

Additionally, Figure 5A and 5C also showed that 4′-Br and 4′-OMe could form an H-bond with the hydroxyl group of Ser-125 and the amino group of Asn-87, which could increase the binding free energy of AChE–the compound. We speculated that similar cases should also exist in the other 4′-halogenated (**8d**, **8g**, **8m**) or 4′-CF_3 compounds (**8p**). This should be the main reason why the 4′-substituted compounds showed the higher anti-AChE activity than both **8a** (R = H) and the 2′- or 3′-substituted isomers.

2.7. Structure-activity relationships

From the data in Table 1 and Figure 3, some important structure-activity relationship for compounds **8** and **7** can be deduced (Fig. 6). (1) In most cases, the aromatic B-ring is very important for the high anti-AChE activity of **8** but disadvantageous for the improvement of the anti-BuChE activity. Seventy-two percent (18/25) and sixty-eight percent (15/22) of the tested **8** showed the higher anti-AChE and lower anti-BuChE activity than their respective **7**, respectively. It was worth noting that for some substitution patterns on the C-ring, the aromatization of the B-ring can increase or reduce the two kinds of activities at the same time (4′-OMe, 2′-Cl, 4′-CF_3, 3′-Me; 2′-Br, 2′-I, 4′-Me, 3′-OMe, 2′,4′-diCl). Additionally, for

2′,6′-difluoro or 2′-F-4′-I substitution pattern, the aromatization of the B-ring can increase the anti-BuChE activity but reduce the anti-AChE activity (**8z** *vs* **7z**; **8ze** *vs* **7ze**). The results indicate that the effect of the aromatization of the B-ring on the activity also depends on the substitution pattern of the C-ring in a few cases.

(2) The substitution pattern of the C-ring dramatically impacts the anti-AChE activity of **8**. Except cyano group (**8s**), all the 4′-substituents can greatly enhance the anti-AChE activity of **8**, whereas the 2′- or 3′-substituents cause reduction of the activity. A similar case also exists in **7**. According to the results of molecular docking above, the enhancement effect of 4′-substituents on the activity should be attributed to the fact that it can form an H-bond with the residues Ser-125 and Asn-87 of AChE and increase the binding free energy of AChE–the compound. Obviously, the 4′ site should be one privileged modifiable position for further structure optimization.

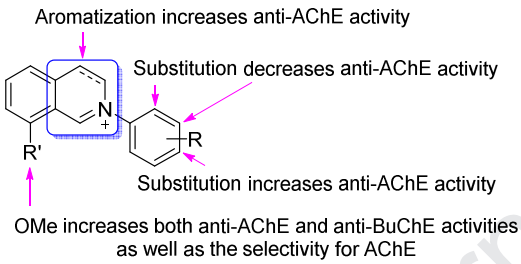

Figure 6. SAR of compounds **8**.

(3) The introduction of 8-OMe can dramatically enhance both anti-AChE and anti-BuChE activities at the same time (**8j** *vs* **8zf**). This result suggests that the substituents on the A-ring can also significantly influence the activity. Therefore, we think that it is necessary to conduct more extensive modification of the A-ring of **8** to find more potent AChE inhibitors in a follow-up study.

(4) For 4′-monohalogenated **8**, the introduction of additional halogen atoms to the C-ring cannot increase anti-AChE activity. All the 2′,4′-dihalogenated **8** were less active on both AChE and BuChE than its respective 4′-monohalogenated compound (Table 1, **8za** *vs* **8g**; **8zc** *vs* **8j**; **8zd** *vs* **8j**; **8ze** *vs* **8m**). A similar case was also observed in compounds **7**. Furthermore, the 2′,6′-difluorinated compound and the 3′,5′-dichlorinated compound also showed the lower anti-AChE activity than the respective monohalogenated compounds, respectively (Table 1, **8z** *vs* **8b**; **8zb** *vs* **8f**).

Journal Pre-proof

Interestingly, the above SAR of **8** for AChE is very similar to that of 2-aryl-β-carbolin-2-ium salts previously reported by us [25]. The reason should be due to the structural similarity between two types of compounds. In fact, **8** can be considered as simple analogues of 2-aryl-β-carbolin-2-niums [24].

3. Conclusions

In summary, we designed and synthesized a series of novel 2-aryl-8-methoxyisoquinol-2-iums (**8**) as the structurally simple analogues of CH. All compounds **8** showed anti-AChE activity at 10 μM, and some of which revealed the excellent activity and high selectivity for AChE, superior to SA, CH and galantamine, a positive drug. **8y** displayed dual AChE−BuChE potent inhibition action. Compounds **8j** and **7j** showed a competitive manner of AChE inhibition. Furthermore, **8** also showed the lower cytotoxicity on normal cells. SAR showed that the B-ring aromatization, the presence of 8-OMe on the A-ring and 4′-substituents on the C-ring are very important for the high anti-AChE activity of **8**. Molecular docking showed that the isoquinoline moiety of **8** can be embedded in a remarkable group of aromatic rings of AChE by the π-π action. These findings will be of great importance for further structural optimization design. Thus, **8** can be considered as promising lead compounds or candidates for the development of novel ChE inhibitor agents.

4. Experimental

4.1. Materials and instruments

Chemicals. Acetylthiocholine iodide (ATCh), butyrylthiocholine iodide (BuTCh), 5,5′-dithio-bis(2-nitrobenzoic acid) (DTNB), and galantamine (>99%) were purchased from Sigma Chemicals Co., Ltd. (Shanghai, China). 2-(3-Methoxyphenyl)acetic acid, 2-phenylethanol and substituted anilines were purchased from Aladdin Industrial Inc. (Shanghai, China). Sanguinarine (SA, >98%) and chelerythrine iodide (CH, >98%) were obtained by isolation from the plant of *M. microcarpa* (Maxim) Fedde in our laboratory [33]. Other reagents and solvents were obtained locally and of analytical grade. The water used was redistilled and ion-free.

Enzymes. AChE (E.C. 3.1.1.7) (BR, 200 u/mg) from fly's head and BuChE (E.C. 3.1.1.8) (BR, 20 u/mg) from horse serum were purchased from Shanghai Yuanye biological technology Co. Ltd (Shanghai, China).

Instruments. ^{1}H and ^{13}C NMR spectra were recorded on an Avance III 500 MHz instrument (Bruker, Karlsruhe, Germany). Chemical shifts were measured relative to the residual solvent peaks of CD_3OD (^{1}H, δ

3.31 ppm; ^{13}C, δ 49.00 ppm). Chemical shifts (δ values) and coupling constants (J values) are given in parts per million and hertz, respectively. High-resolution mass spectra (HR-MS) were carried out with a microTOFQ II instrument (Bruker). Molecular docking analysis was conducted with the Sybyl-X 2.0 software and Discovery Studio 2017 client.

4.2. Chemistry

4.2.1. Synthesis of ***7***

Intermediates **7** were synthesized from commercially available 2-(3-methoxyphenyl)acetic acid as a starting material according to the literature method [27]. **7zf** without 8-OMe was synthesized from commercially available 2-phenylethanol according to the method described in literature [28]. The NMR and MS data were consistent with those previously reported [28].

4.2.2. Synthesis of ***8***

General procedure. To a solution of **7** (0.2 mmol) in a mixture of acetonitrile (30 mL) and toluene (10 mL) was added 5% Pd/C (wetted with ca. 55% water) (0.17 mmol, 80 mg). The mixture was refluxed at 87 °C for about 2 days to complete the reaction. The Pd/C powders in the reaction solution was filtered off through a sand core funnel and completely washed with methanol. The combined solution was concentrated up to dryness under vacuum. The resulted residue was purified by column chromatography over silica (chloroform–methanol-40% HBr aqueous solution, 10:1:0.01) to yield the desired compounds.

*4.2.2.1. 8-Methoxy-2-phenylisoquinolin-2-ium bromide (**8a**)*: Orange-red solid; yield, 67% (0.42 g, 1.34 mmol); ^{1}H NMR (500 MHz, CD_3OD) δ 9.94 (s, 1H), 8.82 (d, J = 6.8 Hz, 1H), 8.58 (d, J = 6.8 Hz, 1H), 8.28 (t, J = 8.1 Hz, 1H), 7.97–7.93 (m, 2H), 7.91 (d, J = 8.2 Hz, 1H), 7.80–7.75 (m, 3H) 7.55 (d, J = 8.2 Hz, 1H), 4.20 (s, 3H); ^{13}C NMR (126 MHz, CD_3OD) δ 159.8, 145.8, 144.4, 141.3, 139.6, 135.9, 132.2, 131.6, 126.9, 125.6, 121.3, 119.7, 111.2, 57.8. HRMS (ESI) m/z calcd for $C_{16}H_{14}NO^+$ $[M–Br]^+$ 236.1070, found 236.1069.

*4.2.2.2. 2-(2-Fluorophenyl)-8-methoxyisoquinolin-2-ium bromide (**8b**)*: Yellow solid; yield, 45% (0.30 g, 0.90 mmol); ^{1}H NMR (500 MHz, CD_3OD) δ 10.05 (s, 1H), 8.75 (d, J = 6.5 Hz, 1H), 8.58 (d, J = 6.7 Hz, 1H), 8.32 (t, J = 8.1 Hz, 1H), 7.97 (t, J = 7.6 Hz, 1H), 7.93 (d, J = 8.2 Hz, 1H), 7.81 (dd, J = 12.6, 7.8 Hz, 1H), 7.63–7.55 (m, 3H), 4.21 (s, 3H); ^{13}C NMR (126 MHz, CD_3OD) δ 160.2, 156.4 (d, J = 253.1 Hz), 148.2, 142.2, 140.1, 137.1, 134.8 (d, J = 8.0 Hz), 133.8 (d, J = 9.2 Hz), 128.7, 127.3 (d, J = 3.9 Hz), 126.7, 121.3, 120.0, 118.6 (d, J = 19.1 Hz), 111.5, 57.9. HRMS (ESI) m/z calcd for $C_{16}H_{13}FNO^+$ $[M–Br]^+$ 254.0976, found 254.0971.

*4.2.2.3. 2-(3-Fluorophenyl)-8-methoxyisoquinolin-2-ium bromide (**8c**)*: Brown solid; yield, 52% (0.35 g, 1.04 mmol); ^{1}H NMR (500 MHz, CD_3OD) δ 9.97 (d, J = 4.4 Hz, 1H), 8.81 (br s, 1H), 8.58 (d, J = 6.7 Hz, 1H), 8.28 (t, J = 7.7 Hz, 1H), 7.90 (d, J = 8.0 Hz, 1H), 7.86 (d, J = 8.5 Hz, 1H), 7.81 (s, 2H), 7.55 (d-like, J = 7.9 Hz, 2H), 4.20 (s, 3H); ^{13}C NMR (126 MHz, CD_3OD) δ 163.8 (d, J = 249.9 Hz), 159.9, 146.1, 145.1 (d, J = 10.1 Hz), 141.6, 139.7, 135.7, 133.4 (d, J = 8.8 Hz), 126.9, 122.0 (d, J = 3.3 Hz), 121.2, 119.7, 119.2 (d, J = 21.2 Hz), 113.7 (d, J = 26.7 Hz), 111.4, 57.9. HRMS (ESI) m/z calcd for $C_{16}H_{13}FNO^+$ $[M–Br]^+$ 254.0976, found 254.0973.

*4.2.2.4. 2-(4-Fluorophenyl)-8-methoxyisoquinolin-2-ium bromide (**8d**)*: Yellow solid; yield, 57% (0.38 g, 1.14 mmol); ^{1}H NMR (500 MHz, CD_3OD) δ 9.98 (s, 1H), 8.82 (d, J = 6.6 Hz, 1H), 8.57 (d, J = 6.6 Hz, 1H), 8.27 (t, J = 8.1 Hz, 1H), 8.03 (dd, J = 8.8, 4.4 Hz, 2H), 7.90 (d, J = 8.0 Hz, 1H), 7.56 (d, J = 8.0 Hz, 1H), 7.51 (t, J = 8.3 Hz, 2H), 4.21 (s, 3H); ^{13}C NMR (126 MHz, CD_3OD) δ 165.1 (d, J = 250.9 Hz), 160.0, 146.4, 141.4, 139.8, 136.3, 128.4 (d, J = 9.3 Hz), 126.9, 121.4, 119.8, 118.4 (d, J = 24.0 Hz), 111.4, 57.8. HRMS (ESI) m/z calcd for $C_{16}H_{13}FNO^+$ $[M–Br]^+$ 254.0975, found 254.0979.

4.2.2.5. 2-(2-Chlorophenyl)-8-methoxyisoquinolin-2-ium bromide (8e): Orange-red solid; yield, 53% (0.38 g, 1.08 mmol); ^{1}H NMR (500 MHz, CD_3OD) δ 10.01 (s, 1H), 8.68 (d, J = 6.4 Hz, 1H), 8.63 (d, J = 6.4 Hz, 1H), 8.34 (t, J = 7.8 Hz, 1H), 8.00 (d, J = 7.6 Hz, 1H), 7.96 (d, J = 8.0 Hz, 1H), 7.85 (d, J = 7.9 Hz, 1H), 7.80 (t, J = 7.7 Hz, 1H), 7.73 (t, J = 7.3 Hz, 1H), 7.60 (d, J = 7.8 Hz, 1H), 4.21 (s, 3H); ^{13}C NMR (126 MHz, CD_3OD) δ 160.1, 148.2, 142.2, 141.3, 140.0, 137.2, 134.2, 132.1, 130.2, 130.0, 129.4, 126.8, 121.1, 120.0, 111.6, 58.0. HRMS (ESI) m/z calcd for $C_{16}H_{13}ClNO^+$ $[M–Br]^+$ 270.0680, found 270.0683.

*4.2.2.6. 2-(3-Chlorophenyl)-8-methoxyisoquinolin-2-ium bromide (**8f**)*: Brown solid; yield, 58% (0.41 g, 1.42 mmol); ^{1}H NMR (500 MHz, CD_3OD) δ 10.06 (s, 1H), 8.89 (d, J = 6.9 Hz, 1H), 8.59 (d, J = 6.9 Hz, 1H), 8.50 (s, 1H), 8.34 (d, J = 7.9 Hz, 1H), 8.29 (d, J = 8.0 Hz, 1H), 8.19 (d, J = 8.0 Hz, 1H), 7.94–7.91 (m, 2H), 7.57 (d, J = 8.1 Hz, 1H), 4.21 (s, 3H); ^{13}C NMR (126 MHz, CD_3OD) δ 160.2, 146.6, 145.5, 141.7, 140.0, 136.9, 136.0, 133.0, 132.5, 126.9, 126.4, 124.7, 121.5, 119.9, 111.4, 57.8. HRMS (ESI) m/z calcd for $C_{16}H_{13}ClNO^+$ $[M–Br]^+$ 270.0680, found 270.0678.

*4.2.2.7. 2-(4-Chlorophenyl)-8-methoxyisoquinolin-2-ium bromide (**8g**)*: Yellow solid; yield, 61% (0.43 g, 1.50 mmol); ^{1}H NMR (500 MHz, CD_3OD) δ 10.03 (s, 1H), 8.83 (dd, J = 6.9, 1.7 Hz, 1H), 8.55 (d, J = 6.8 Hz, 1H), 8.28 (t, J = 8.2 Hz, 1H), 7.93 (d, J = 8.9 Hz, 2H), 7.90 (d, J = 8.3 Hz, 1H), 7.79 (d, J = 8.9 Hz, 2H), 7.56 (d, J = 8.1 Hz, 1H),

4.21 (s, 3H); ^{13}C NMR (126 MHz, CD_3OD) δ 160.2, 146.6, 143.3, 141.5, 140.0, 138.5, 136.1, 131.7, 127.6, 126.8, 121.5, 119.9, 111.3, 57.6. HRMS (ESI) *m*/*z* calcd for $C_{16}H_{13}ClNO^+$ $[M–Br]^+$ 270.0680, found 270.0660.

*4.2.2.8. 2-(2-Bromophenyl)-8-methoxyisoquinolin-2-ium bromide (**8h**)*: Orange-red solid; yield, 44% (0.35 g, 0.88 mmol); ^{1}H NMR (500 MHz, CD_3OD) δ 9.98–9.92 (m, 1H), 8.64 (s, 2H), 8.34 (t-like, *J* = 7.8 Hz, 1H), 7.99–7.95 (m, 3H), 7.77–7.71 (m, 2H), 7.60 (d, *J* = 7.5 Hz, 1H), 4.20 (s, 3H); ^{13}C NMR (126 MHz, CD_3OD) δ 159.9, 147.9, 142.7, 142.2, 139.9, 137.0, 135.2, 134.4, 130.8, 129.3, 126.8, 120.9, 119.9, 119.4, 111.6, 58.1. HRMS (ESI) *m*/*z* calcd for $C_{16}H_{13}BrNO^+$ $[M–Br]^+$ 314.0175, 316.0155, found 314.0174, 316.0154.

*4.2.2.9. 2-(3-Bromophenyl)-8-methoxyisoquinolin-2-ium bromide (**8i**)*: Brown solid; yield, 55% (0.43 g, 1.10 mmol); ^{1}H NMR (500 MHz, CD_3OD) δ 10.98 (s, 1H), 8.80 (d, *J* = 5.7 Hz, 1H), 8.57 (d, *J* = 5.9 Hz, 1H), 8.29 (t, *J* = 7.6 Hz, 1H), 8.21 (s, 1H), 7.95 (d, *J* = 7.4 Hz, 1H), 7.92 (t, *J* = 8.5 Hz, 2H), 7.70 (t-like, 1H), 7.56 (d, *J* = 7.6 Hz, 1H), 4.21 (s, 3H); ^{13}C NMR (126 MHz, CD_3OD) δ 160.1, 146.4, 145.3, 141.6, 139.9, 135.9, 135.4, 133.2, 129.0, 126.9, 125.1, 124.3, 121.4, 119.8, 111.4, 57.8. HRMS (ESI) *m*/*z* calcd for $C_{16}H_{13}BrNO^+$ $[M–Br]^+$ 314.0175, 316.0155, found 314.0177, 316.0153.

*4.2.2.10. 2-(4-Bromophenyl)-8-methoxyisoquinolin-2-ium bromide (**8j**)*: Brown solid; yield, 63% (0.50 g, 1.26 mmol); ^{1}H NMR (500 MHz, CD_3OD) δ 10.02 (s, 1H), 8.82 (dd, *J* = 6.9, 1.5 Hz, 1H), 8.54 (d, *J* = 6.9 Hz, 1H), 8.28 (t, *J* = 8.1 Hz, 1H), 7.93 (d, *J* = 8.7 Hz, 2H), 7.89 (d, *J* = 8.2 Hz, 1H), 7.85 (d, *J* = 8.4 Hz, 2H), 7.55 (d, *J* = 8.1 Hz, 1H), 4.21 (s, 3H); ^{13}C NMR (126 MHz, CD_3OD) δ 160.2, 146.5, 141.6, 140.0, 136.0, 134.8, 134.4, 127.8, 126.9, 126.5, 121.5, 119.9, 111.3, 57.6. HRMS (ESI) *m*/*z* calcd for $C_{16}H_{13}BrNO^+$ $[M–Br]^+$ 314.0175, 316.0155, found 314.0174, 316.0158.

*4.2.2.11. 2-(2-Iodophenyl)-8-methoxyisoquinolin-2-ium bromide (**8k**)*: Yellow solid; yield, 40% (0.35 g, 0.80 mmol); ^{1}H NMR (500 MHz, CD_3OD) δ 10.01 (d, *J* = 1.3 Hz, 1H), 8.65 (dd, *J* = 6.9, 1.4 Hz, 1H), 8.60 (t, *J* = 6.9 Hz, 1H), 8.33 (t, *J* = 8.2 Hz, 1H), 8.21 (dd, *J* = 8.0, 1.3 Hz, 1H), 7.95 (d, *J* = 8.2 Hz, 1H), 7.87 (dt, *J* = 8.0, 1.4 Hz, 1H), 7.76 (dt, *J* = 7.7, 1.3 Hz, 1H), 7.59 (d, *J* = 8.1 Hz, 1H), 7.51 (dt, *J* = 7.8, 1.5 Hz, 1H), 4.21 (s, 3H); ^{13}C NMR (126 MHz, CD_3OD) δ 160.4, 148.4, 146.9, 142.1, 141.7, 140.4, 137.3, 134.1, 131.4, 128.4, 126.8, 121.3, 120.1, 111.5, 95.1, 57.7. HRMS (ESI) *m*/*z* calcd for $C_{16}H_{13}INO^+$ $[M–Br]^+$ 362.0036, found 362.0014.

*4.2.2.12. 2-(3-Iodophenyl)-8-methoxyisoquinolin-2-ium bromide (**8l**)*: Orange-red solid; yield, 51% (0.45 g, 1.02 mmol); ^{1}H NMR (500 MHz, CD_3OD) δ 9.94 (s, 1H), 8.78 (d, *J* = 6.3 Hz, 1H), 8.56 (d, *J* = 6.6 Hz, 1H), 8.34 (s, 1H),

8.28 (t, *J* = 8.0 Hz, 1H), 8.10 (d, *J* = 7.7 Hz, 1H), 7.97 (d, *J* = 7.6 Hz, 1H), 7.90 (d, *J* = 8.1 Hz, 1H), 7.58–7.51 (m, 2H), 4.20 (3H, s); ^{13}C NMR (126 MHz, CD_3OD) δ 159.9, 146.2, 145.0, 141.5, 141.3, 139.7, 135.8, 134.4, 133.0, 126.9, 125.4, 121.3, 119.7, 111.3, 95.6, 57.9. HRMS (ESI) *m*/*z* calcd for $C_{16}H_{13}INO^+$ $[M–Br]^+$ 362.0036, found 362.0042.

*4.2.2.13. 2-(4-Iodophenyl)-8-methoxyisoquinolin-2-ium bromide (**8m**)*: Yellow solid; yield, 57% (0.50 g, 1.14 mmol); ^{1}H NMR (500 MHz, CD_3OD) δ 10.01 (s, 1H), 8.82 (d, *J* = 6.6 Hz, 1H), 8.55 (d, *J* = 6.8 Hz, 1H), 8.28 (t, *J* = 8.1 Hz, 1H), 8.13 (d, *J* = 8.4 Hz, 2H), 7.90 (d, *J* = 8.2 Hz, 1H), 7.72 (d, *J* = 8.4 Hz, 2H), 7.56 (d, *J* = 8.1 Hz, 1H), 4.21 (s, 3H); ^{13}C NMR (126 MHz, CD_3OD) δ 160.2, 146.4, 144.3, 141.5, 140.9, 140.0, 136.0, 127.7, 126.9, 121.5, 119.9, 111.3, 98.2, 57.7. HRMS (ESI) *m*/*z* calcd for $C_{16}H_{13}INO^+$ $[M–Br]^+$ 362.0036, found 362.0028.

*4.2.2.14. 8-Methoxy-2-(2-trifluorophenyl)isoquinolin-2-ium bromide (**8n**)*: Brown solid; yield, 41% (0.32 g, 0.82 mmol); ^{1}H NMR (500 MHz, CD_3OD) δ 10.15 (s, 1H), 8.75 (d, *J* = 6.6 Hz, 1H), 8.60 (d, *J* = 6.4 Hz, 1H), 8.36 (t, *J* = 8.1 Hz, 1H), 8.11 (d, *J* = 7.2 Hz, 1H), 8.06–8.00 (m, 3H), 7.98 (d, *J* = 8.2 Hz, 1H), 7.62 (d, *J* = 8.1 Hz, 1H), 4.20 (s, 3H); ^{13}C NMR (126 MHz, CD_3OD) δ 160.3, 148.7, 142.5, 140.9, 140.3 , 137.5, 135.7, 133.7, 130.3, 129.0 (q, *J* = 4.1 Hz), 126.4, 126.3, 124.0 (q, *J* = 272.0 Hz), 120.8, 120.1, 111.8, 56.6. HRMS (ESI) *m*/*z* calcd for $C_{17}H_{13}F_3NO^+$ $[M–Br]^+$ 304.0944, found 304.0940.

*4.2.2.15. 8-Methoxy-2-(3-trifluorophenyl)isoquinolin-2-ium bromide (**8o**)*: Yellow solid; yield, 59% (0.45 g, 1.18 mmol); ^{1}H NMR (500 MHz, CD_3OD) δ 10.08 (s, 1H), 8.87 (d, *J* = 6.4 Hz, 1H), 8.59 (d, *J* = 6.5 Hz, 1H), 8.35 (s, 1H), 8.30 (t, *J* = 8.0 Hz, 1H), 8.25 (d, *J* = 7.5 Hz, 1H), 8.09 (d, *J* = 7.6 Hz, 1H), 8.01 (t, *J* = 7.7 Hz, 1H), 7.92 (d, *J* = 8.1 Hz, 1H), 7.58 (d, *J* = 8.0 Hz, 1H), 4.22 (s, 3H); ^{13}C NMR (126 MHz, CD_3OD) δ 160.3, 147.0, 145.0, 141.8, 140.1, 136.2, 133.5 (q, *J* = 33.2 Hz), 132.9, 130.1, 129.1 (q, *J* = 3.2 Hz), 127.0, 124.1 (q, *J* = 27.0 Hz), 122.1 (q, *J* = 3.6 Hz), 121.5, 119.9, 111.4, 57.8. HRMS (ESI) *m*/*z* calcd for $C_{17}H_{13}F_3NO^+$ $[M–Br]^+$ 304.0944, found 304.0945.

*4.2.2.16. 8-Methoxy-2-(4-trifluorophenyl)isoquinolin-2-ium bromide (**8p**)*: Orange-red solid; yield, 61% (0.47 g, 1.22 mmol); ^{1}H NMR (500 MHz, CD_3OD) δ 10.10 (s, 1H), 8.87 (br s, 1H), 8.57 (br s, 1H), 8.29 (t, *J* = 6.7 Hz, 1H), 8.15 (s-like, 2H), 8.10 (s-like, 2H), 7.91 (d, *J* = 7.3 Hz, 1H), 7.57 (d, *J* = 7.2 Hz, 1H), 4.22 (s, 3H); ^{13}C NMR (126 MHz, CD_3OD) δ 160.3, 147.2, 147.0, 141.9, 140.2, 136.1, 134.0 (d, *J* = 32.9 Hz), 128.7 (d-like, *J* = 3.6 Hz), 127.3, 127.0, 124.8 (d, *J* = 270.6 Hz), 121.5, 120.0, 111.5, 57.8. HRMS (ESI) *m*/*z* calcd for $C_{17}H_{13}F_3NO^+$ $[M–Br]^+$ 304.0944, found 304.0940.

Journal Pre-proof

*4.2.2.17. 2-(2-Cyanophenyl)-8-methoxyisoquinolin-2-ium bromide (**8q**)*: Yellow solid; yield, 42% (0.29 g, 0.84 mmol); ^{1}H NMR (500 MHz, CD_3OD) δ 10.25 (s, 1H), 8.86 (d-like, J = 5.9 Hz, 1H), 8.62 (d-like, J = 5.6 Hz, 1H), 8.35 (t, J = 7.7 Hz, 1H), 8.15 (d, J = 7.3 Hz, 1H), 8.09 (br s, 2H), 7.95 (d-like, J = 7.5 Hz, 2H), 7.60 (d, J = 7.6 Hz, 1H), 4.22 (s, 3H); ^{13}C NMR (126 MHz, CD_3OD) δ 160.6, 148.4, 145.4, 142.6, 140.4, 136.8, 136.4, 135.7, 133.3, 128.9, 126.9, 121.3, 120.1, 115.4, 111.8, 111.1, 57.9. HRMS (ESI) m/z calcd for $C_{17}H_{13}N_2O^+$ $[M–Br]^+$ 261.1022, found 261.1023.

*4.2.2.18. 2-(3-Cyanophenyl)-8-methoxyisoquinolin-2-ium bromide (**8r**)*: Yellow solid; yield, 54% (0.37 g, 1.08 mmol); ^{1}H NMR (500 MHz, CD_3OD) δ 10.10 (br s, 1H), 8.87 (s, 1H), 8.58–7.91 (m, 7H), 7.57 (s, 1H), 4.23 (s, 3H); ^{13}C NMR (126 MHz, CD_3OD) ^{13}C NMR (126 MHz, CD_3OD) δ 160.2, 147.5, 144.8, 144.7, 142.0, 141.7, 140.1, 140.0, 136.3, 135.9, 133.0, 132.1, 131.3, 130.4, 127.2, 127.1, 121.5, 120.0, 115.3, 111.6, 111.5, 58.3, 58.2. HRMS (ESI) m/z calcd for $C_{17}H_{13}N_2O^+$ $[M–Br]^+$ 261.1022, found 261.1018.

*4.2.2.19. 2-(4-Cyanophenyl)-8-methoxyisoquinolin-2-ium bromide (**8s**)*: Yellow solid; yield, 55% (0.38 g, 1.10 mmol); ^{1}H NMR (500 MHz, CD_3OD) δ 10.07 (br s, 1H), 8.89 (d, J = 6.6 Hz, 1H), 8.59 (d, J = 6.6 Hz, 1H), 8.38–8.06 (m, 5H), 7.92 (d, J = 8.1 Hz, 1H), 7.58 (t, J = 8.1 Hz, 1H), 4.22 (s, 3H); ^{13}C NMR (126 MHz, CD_3OD) δ 160.2, 146.6, 145.5, 141.7, 140.0, 136.9, 136.0, 133.0, 132.5, 126.9, 126.3, 124.7, 121.5, 119.9, 111.4, 57.8. HRMS (ESI) m/z calcd for $C_{17}H_{13}N_2O^+$ $[M–Br]^+$ 261.1022, found 261.1016.

*4.2.2.20. 8-Methoxy-2-(o-toly)isoquinolin-2-ium bromide (**8t**)*: Orange red solid; yield, 40% (0.26 g, 0.80 mmol); ^{1}H NMR (500 MHz, CD_3OD) δ 9.94 (s, 1H), 8.67 (d, J = 6.4 Hz, 1H), 8.62 (d, J = 6.3 Hz, 1H), 8.31 (t, J = 7.9 Hz, 1H), 7.95 (d, J = 7.9 Hz, 1H), 7.71 (d, J = 7.6 Hz, 1H), 7.66 (t, J = 7.2 Hz, 1H), 7.62–7.52 (m, 3H), 4.21 (s, 3H), 2.24 (s, 3H); ^{13}C NMR (126 MHz, CD_3OD) δ 160.0, 147.4, 143.8, 141.5, 140.0, 137.2, 134.1, 133.1, 132.6, 128.9, 127.3, 126.9, 121.4, 120.0, 111.4, 57.9, 17.5. HRMS (ESI) m/z calcd for $C_{17}H_{16}NO^+$ $[M–Br]^+$ 250.1226, found 250.1229.

*4.2.2.21. 8-Methoxy-2-(m-toly)isoquinolin-2-ium bromide (**8u**)*: Brown solid; yield, 52% (0.34 g, 1.04 mmol); ^{1}H NMR (500 MHz, CD_3OD) δ 9.92 (s, 1H), 8.82 (d, J = 5.9 Hz, 1H), 8.57 (d, J = 6.0 Hz, 1H), 8.26 (t, J = 7.7 Hz, 1H), 7.89 (d, J = 7.8 Hz, 1H), 7.79 (s, 1H), 7.73 (d, J = 7.1 Hz, 1H), 7.64 (t, J = 7.3 Hz, 1H), 7.56 (t-like, J = 7.2 Hz, 2H), 4.21 (s, 3H), 2.54 (s, 3H); ^{13}C NMR (126 MHz, CD_3OD) δ 159.8, 145.8, 144.4, 142.4, 141.2, 139.6, 136.0, 132.9, 131.4, 126.9, 126.1, 122.7, 121.3, 119.8, 111.3, 57.9, 21.4. HRMS (ESI) m/z calcd for $C_{17}H_{16}NO^+$ $[M–Br]^+$ 250.1226, found 250.1228.

Journal Pre-proof

*4.2.2.22. 8-Methoxy-2-(p-toly)isoquinolin-2-ium bromide (**8v**)*: Golden yellow solid; yield, 61% (0.40 g, 1.22 mmol); ^{1}H NMR (500 MHz, CD_3OD) δ 9.27 (s, 1H), 7.94–7.52 (m, 5H), 7.46 (d-like, J = 5.7 Hz, 2H), 7.21 (d, *J* = 5.7 Hz, 1H), 7.09 (d, *J* = 6.1 Hz, 1H), 4.05 (s, 3H), 2.44 (s, 3H); ^{13}C NMR (126 MHz, CD_3OD) δ 163.8, 161.8, 142.72, 142.67, 142.3, 139.6, 132.1, 131.7, 125.6, 123.5, 121.2, 116.0, 112.4, 57.7, 21.3. HRMS (ESI) *m*/*z* calcd for $C_{17}H_{16}NO^+$ $[M–Br]^+$ 250.1226, found 250.1228.

*4.2.2.23. 8-Methoxy-2-(2-methoxyphenyl)isoquinolin-2-ium bromide (**8w**)*: Golden yellow solid; yield, 40% (0.28 g, 0.80 mmol); H: ^{1}H NMR (500 MHz, CD_3OD) δ 9.90 (s, 1H), 8.64 (d, *J* = 6.6 Hz, 1H), 8.54–8.51 (m, 1H), 8.28 (t, *J* = 8.0 Hz, 1H), 7.90 (d, *J* = 8.1 Hz, 1H), 7.77 (d, *J* = 7.4 Hz, 1H), 7.73 (t, *J* = 8.0 Hz, 1H), 7.55 (d, *J* = 8.0 Hz, 1H), 7.44 (d, *J* = 8.3 Hz, 1H), 7.29 (t, *J* = 7.6 Hz, 1H), 4.19 (s, 3H), 3.92 (s, 3H). ^{13}C NMR (126 MHz, CD_3OD) δ 159.9, 153.7, 148.1, 141.5, 139.9, 137.9, 134.2, 133.0, 128.0, 126.3, 122.6, 121.2, 119.9, 114.4, 111.2, 57.8, 57.2. HRMS (ESI) *m*/*z* calcd for $C_{17}H_{16}NO_2^+$ $[M–Br]^+$ 266.1176, found 266.1164.

*4.2.2.24. 8-Methoxy-2-(3-methoxyphenyl)isoquinolin-2-ium bromide (**8x**)*: Brown solid; yield, 45% (0.31 g, 0.90 mmol); ^{1}H NMR (500 MHz, CD_3OD) δ 9.95 (s, 1H), 8.82 (d, *J* = 5.8 Hz, 1H), 8.55 (d, *J* = 5.8 Hz, 1H), 8.26 (t, *J* = 7.8 Hz, 1H), 7.89 (d, *J* = 7.6 Hz, 1H), 7.65 (t, *J* = 7.8 Hz, 1H), 7.55 (d, *J* = 7.8 Hz, 1H), 7.52 (s, 1H), 7.46 (d, *J* = 7.4 Hz, 1H), 7.29 (d, *J* = 8.1 Hz, 1H), 4.20 (s, 3H), 3.95 (s, 3H); ^{13}C NMR (126 MHz, CD_3OD) δ 162.3, 160.0, 146.1, 145.6, 141.3, 139.9, 136.2, 132.5, 126.8, 121.4, 119.8, 118.3, 117.7, 111.4, 111.3, 57.7, 56.8. HRMS (ESI) *m*/*z* calcd for $C_{17}H_{16}NO_2^+$ $[M–Br]^+$ 266.1176, found 266.1182.

*4.2.2.25. 8-Methoxy-2-(4-methoxyphenyl)isoquinolin-2-ium bromide (**8y**)*: Brown red solid; yield, 59% (0.41 g, 1.18 mmol); ^{1}H NMR (500 MHz, CD_3OD) δ 9.90 (s, 1H), 8.80 (d, *J* = 6.2 Hz, 1H), 8.54 (d, *J* = 6.2 Hz, 1H), 8.24 (t, *J* = 7.8 Hz, 1H), 7.88 (t, *J* = 8.2 Hz, 3H), 7.54 (d, *J* = 7.8 Hz, 1H), 7.26 (d, *J* = 7.5 Hz, 2H), 4.21 (s, 3H), 3.93 (s, 3H); ^{13}C NMR (126 MHz, CD_3OD) δ 163.0, 159.8, 145.8, 141.0, 139.5, 137.6, 136.4, 127.2, 126.9, 121.5, 119.8, 116.7, 111.3, 57.9, 56.7. HRMS (ESI) *m*/*z* calcd for $C_{17}H_{16}NO_2^+$ $[M–Br]^+$ 266.1176, found 266.1181.

*4.2.2.26. 2-(2,6-Difluorophenyl)-8-methoxyisoquinolin-2-ium bromide (**8z**)*: Yellow solid; yield, 54% (0.38 g, 1.08 mmol); ^{1}H NMR (500 MHz, CD_3OD) δ 10.06 (s, 1H), 8.89 (d, *J* = 6.5 Hz, 1H), 8.58 (d, *J* = 6.6 Hz, 1H), 8.50 (s, 1H), 8.33 (d, *J* = 7.5 Hz, 1H), 8.29 (t, *J* = 8.0 Hz, 1H), 8.19 (d, *J* = 7.7 Hz, 1H), 7.95–7.89 (m, 2H), 7.56 (d, *J* = 7.9 Hz, 1H), 4.21 (s, 3H); ^{13}C NMR (126 MHz, CD_3OD) δ 160.2, 157.6 (d, *J* = 253.5 Hz), 149.3, 143.0, 140.1, 137.4,

Journal Pre-proof

135.3 (t, *J* = 9.7 Hz), 129.7, 126.9, 121.1, 120.0, 114.3 (dd, *J* = 18.9, 3.4, Hz), 111.8, 57.9. HRMS (ESI) *m*/*z* calcd for $C_{16}H_{12}F_2NO^+$ $[M–Br]^+$ 272.0881, found 272.0884.

*4.2.2.27. 2-(2,4-Dichlorophenyl)-8-methoxyisoquinolin-2-ium bromide (**8za**)*: Brown solid; yield, 53% (0.41 g, 1.06 mmol); ^{1}H NMR (500 MHz, CD_3OD) δ 10.02 (s, 1H), 8.67 (br s, 1H), 8.63 (br s, 1H), 8.34 (t, *J* = 7.4 Hz, 1H), 8.03 (d, *J* = 7.7 Hz, 1H), 7.95 (d, *J* = 7.5 Hz, 1H), 7.90 (s, 1H), 7.73 (d, *J* = 7.3 Hz, 1H), 7.60 (d, *J* = 7.6 Hz, 1H), 4.20 (3H, s, 1H); ^{13}C NMR (126 MHz, CD_3OD) δ 160.0, 148.0, 142.3, 139.9, 139.7, 139.0, 136.8, 131.6, 131.2, 130.4, 130.2, 126.7, 120.9, 119.8, 111.5, 57.9. HRMS (ESI) *m*/*z* calcd for $C_{16}H_{12}Cl_2NO^+$ $[M–Br]^+$ 304.0290, found 304,0294.

*4.2.2.28. 2-(3,5-Dichlorophenyl)-8-methoxyisoquinolin-2-ium bromide (**8zb**)*: Orange-red solid; yield, 57% (0.44 g, 1.14 mmol); ^{1}H NMR (500 MHz, CD_3OD) δ 10.06 (s, 1H), 8.82 (br s, 1H), 8.56 (br s, 1H), 8.29 (t, *J* = 7.9 Hz, 1H), 8.07 (s, 2H), 7.91 (d, *J* = 7.2 Hz, 1H), 7.87 (s, 1H), 7.57 (d, *J* = 6.9 Hz, 1H), 4.22 (s, 3H); ^{13}C NMR (126 MHz, CD_3OD) δ 160.4, 147.2, 145.8, 142.0, 140.2, 137.6, 136.0, 132.3, 126.9, 125.6, 121.4, 119.9, 111.5, 58.0. HRMS (ESI) *m*/*z* calcd for $C_{16}H_{12}Cl_2NO^+$ $[M–Br]^+$ 304.0290, found 304,0297.

*4.2.2.29. 2-(2,4-Dibromophenyl)-8-methoxyisoquinolin-2-ium bromide (**8zc**)*: Golden yellow solid; yield, 55% (0.52 g, 1.10 mmol); ^{1}H NMR (500 MHz, CD_3OD) δ 10.08 (s, 1H), 8.68 (br, s, 1H), 8.61 (br s, 1H), 8.34 (t-like, 1H), 8.21 (s, 1H), 7.95–7.91 (m, 3H), 7.59 (d, *J* = 7.0 Hz, 1H), 4.21 (s, 3H); ^{13}C NMR (126 MHz, CD_3OD) δ 160.3, 148.5, 142.4, 142.3, 140.3, 137.6, 137.1, 133.9, 130.8, 127.2, 126.8, 121.2, 121.0, 120.1, 111.6, 58.0. HRMS (ESI) *m*/*z* calcd for $C_{16}H_{12}Br_2NO^+$ $[M-Br]^+$ 391.9280, found 391.9279.

*4.2.2.30. 2-(4-Bromo-2-fluorophenyl)-8-methoxyisoquinolin-2-ium bromide (**8zd**)*: Orange-red solid; yield, 50% (0.41 g, 1.00 mmol); ^{1}H NMR (500 MHz, CD_3OD) δ 10.09 (s, 1H), 8.77 (br s, 1H), 8.58 (br s, 1H), 8.32 (t-like, 1H), 7.97–7.90 (m, 2H), 7.87 (d, *J* = 9.4 Hz, 1H), 7.77 (br s, 1H), 7.58 (d, *J* = 7.0 Hz, 1H), 4.22 (s, 3H); ^{13}C NMR (126 MHz, CD_3OD) δ 160.3, 156.8 (d, *J* = 254.8 Hz), 148.6, 142.3, 140.2, 137.1, 1231.2 (d, *J* = 10.9 Hz 1H), 129.3 (d, *J* = 3.7 Hz), 130.3, 127.2 (d, *J* = 9.0 Hz), 126.8, 122.2 (d, *J* = 22.0 Hz), 121.4, 120.0, 111.6, 58.0. HRMS (ESI) *m*/*z* calcd for $C_{16}H_{12}FBrNO^+$ $[M–Br]^+$ 332.0081, found 332.0067.

*4.2.2.31. 2-(2-Fluoro-4-iodophenyl)-8-methoxyisoquinolin-2-ium bromide (**8ze**)*: Brown solid; yield, 60% (0.55 g, 1.20 mmol); ^{1}H NMR (500 MHz, CD_3OD) δ 10.06 (s, 1H), 8.75 (br s, 1H), 8.58 (br s, 1H), 8.32 (t-like, *J* = 7.8 Hz, 1H), 7.99 (d, *J* = 9.2 Hz, 1H), 7.96-7.90 (m, 2H), 7.76 (br s, 1H), 7.58 (d, *J* = 7.3 Hz, 1H), 4.21 (s, 3H); ^{13}C NMR (126

Journal Pre-proof

MHz, CD_3OD) δ 160.2, 155.8 (d, *J* = 257.1 Hz), 148.3, 142.3, 140.1, 136.9, 136.6 (d, *J* = 3.6 Hz), 131.6 (d, *J* = 12.2 Hz), 130.1, 127.8 (d, *J* = 21.4 Hz), 126.8, 121.3, 120.0, 111.6, 98.7 (d, *J* = 7.9 Hz), 58.0. HRMS (ESI) *m*/*z* calcd for $C_{16}H_{12}FINO^+$ $[M–Br]^+$ 379.9942, found 379.9936.

*4.2.2.32. 2-(4-Bromophenyl)isoquinolin-2-ium bromide (**8zf**)*: White solid; yield, 76% (0.55 g, 1.52 mmol); ^1H NMR (500 MHz, CD_3OD) δ 10.25 (s, 1H), 8.91 (d, *J* = 6.8 Hz, 1H), 8.66 (t, *J* = 7.4 Hz, 2H), 8.43 (d, *J* = 8.3 Hz, 1H), 8.35 (t, *J* = 7.6 Hz, 1H), 8.15 (t, *J* = 7.6 Hz, 1H), 7.96 (d, *J* = 8.7 Hz, 2H), 7.91 (d, *J* = 8.7 Hz, 2H); ^{13}C NMR (126 MHz, CD_3OD) δ 151.2, 143.6, 139.4, 139.3, 135.7, 134.8, 133.0, 132.5, 129.2, 128.7, 127.7, 127.6, 126.7. HRMS (ESI) *m*/*z* calcd for $C_{15}H_{11}BrN^+$ $[M–Br]^+$ 284.0069, found 284.0076.

4.3. Assay of AChE and BuChE inhibition activity

The Ellman's coupled enzyme method [29] as described previously [25], was used to assay the inhibitory activity of compounds against AChE. Briefly, 90 μL potassium phosphate buffer (PBS, 0.1 M, pH 7.4), 10 μL the solution of AChE (2 units/mL) in 0.1 M PBS (pH 7.4) and 10 μL the solution of test compounds (200 μM) in the mixed solution of methanol-PBS (pH 7.4) (1:9, V/V) were added to each well of a 96-well plate. The methanol-PBS solution was used as a blank control. After incubation at room temperature for 10 min, 60 μL the solution of 10 mM DTNB in PBS was added into each the well. The plate was placed on crushed ices and cooled for 20 min. To each the well was added 30 μL the solution of ATCh (7.5 mM) in PBS (pH 7.4). After incubation at 37 °C for 40 min, the initial rate of the enzyme reaction was analyzed by measuring absorbance at wavelength of 412 nm with a microplate reader (Molecular Devices Co., Ltd.). Each test was performed in triplicate. Inhibition rates of the enzyme were calculated relative to a control sample. The inhibitory activity against BuChE were measured as described above for AChE, using BuChE (0.7 unit/mL) and BuTCh (4 mM) instead of AChE and ATCh as the enzyme and substrate, respectively.

The IC_{50} values of compounds were measured according to the same method as above. A series of concentrations of the compound were set on the base of the screening results and used to test the inhibition rate against AChE or BuChE. The probit value of the inhibition rate for each the concentration and the corresponding lg[concentration] were used to conduct linear regression by the linear least-square fitting method. IC_{50} values and 95% confidence intervals were calculated from the regression equations by using PRISM software ver. 5.0 (GraphPad Software Inc., San Diego, CA, USA).

4.4. Cytotoxicity Assay

The cytotoxicity of compounds **8j**, **8y**, **8zc**, **7j**, **7y** and **7zc** was assayed using the MTT method. Mouse neuroblastoma N2a cells, primary cultured porcine fetal kidney cells and primary cultured goat fetal fibroblast were used as the test cells. The operation procedure was descripted in supporting information.

4.5. Molecular Docking Study

Molecular docking simulations were performed using the software Autodock 4.2 along with AutoDock Tools (ADT 1.5.6) using the hybrid Lamarckian Genetic Algorithm (LGA). The three dimensional (3D) crystal structures of AChE (PDB code: 4BDT) and BuChE (PDB code: 5K5E) were obtained from the RCSB Protein Data Bank. The standard 3D structure (mol2 format) of all compounds were constructed by using the "SKETCH" option function in SYBYL-X. The other details were descripted in supporting information.

Conflicts of interest

The authors state no conflict of interest.

Acknowledgements

This work was financially supported by the National Natural Science Foundation of China (No. 31872008) and the Key Research and Development Project of Shaanxi Province (2019NY-195).

Appendix A. Supplementary data

Supplementary information (^{1}H NMR, ^{13}C NMR and HRMS spectra, cytotoxicity assay and molecular docking study) to this article can be found online at https://doi.org/xxx.

Author Contributions

Conceptualization: LZ.
Data curation: BZ HL.
Formal analysis: BL.
Funding acquisition: LZ.
Investigation: BZ HL ZC DL.
Methodology: LZ.
Project administration: LZ HG.
Resources: LZ.
Supervision: LZ JG HG.
Validation: LZ.
Visualization: BZ LZ DL.

Writing – original draft: BH LZ HG.

Writing – review & editing: LZ JG.

Journal Pre-proof

Journal Pre-proof

References

[1] M.M. Mesulam, A. Guillozet, P. Shaw, A. Levey, E.G. Duysen, O. Lockridge, Acetylcholinesterase knockouts establish central cholinergic pathways and can use butyrylcholinesterase to hydrolyze acetylcholine, Neuroscience 110 (2002) 627–639.

[2] A. Chatonnet, O. Lockridge, Comparison of butyrylcholinesterase and acetylcholinesterase, Biochem. J. 260 (1989) 625–634.

[3] Q. Li, H. Yang, Y. Chen, H. Sun, Recent progress in the identification of selective butyrylcholinesterase inhibitors for Alzheimer's disease, Eur. J. Med. Chem. 132 (2017) 294–309.

[4] A. Rampa, A. Bisi, F. Belluti, S. Gobbi, P. Valenti, V. Andrisano, V. Cavrini, A. Cavalli, M. Recanatini, Acetylcholinesterase inhibitors for potential use in Alzheimer's disease: molecular modeling, synthesis and kinetic evaluation of 11H-indeno-[1,2-b]-quinolin-10-ylamine derivatives, Bioorg. Med. Chem. 8 (2000), 497–506.

[5] M.A. Khorshid, A.M. Fatma Hassan, A.M. Mona Abd El-Gawad, A.K. Enab, Effect of some plants and pesticides on acetylcholinesterase, Am. J. Food Technol. 10 (2015) 93–99.

[6] C. Zhang, Q.Y. Du, L.D. Chen, W.H. Wu, S.Y. Liao, L.H. Yu, X.T. Liang, Design, synthesis and evaluation of novel tacrine-multialkoxybenzene hybrids as multi-targeted compounds against Alzheimer's disease, Eur. J. Med. Chem. 116 (2016) 200–209.

[7] M. Prince, A. Comas-Herrera, M. Knapp, M. Guerchet, M. Karagiannidou, World Alzheimer Report 2016 in Alzheimer's Disease International, 2016.

[8] V.N. Talesa, Acetylcholinesterase in Alzheimer's disease, Mech. Ageing Dev. 122 (2001) 1961–1969.

[9] J. Hardy, The amyloid hypothesis for Alzheimer's disease: a critical reappraisal, J. Neurochem. 110 (2009) 1129–1134.

[10] I. Grundke-Iqbal, K. Iqbal, Y.C. Tung, M. Quinlan, H.M. Wisniewski, L.I. Binder, Abnormal phosphorylation of the microtubule-associated protein tau (t) in Alzheimer cytoskeletal pathology, Proc. Natl. Acad. Sci. U. S. A. 83 (1986) 4913–4917.

[11] M. Rosini, E. Simoni, A. Milelli, A. Minarini, C. Melchiorre, Oxidative stress in Alzheimer's disease: are we connecting the dots? J. Med. Chem. 57 (2014) 2821–2831.

[12] R.T. Bartus, On neurodegenerative diseases, models, and treatment strategies: lessons learned and lessons forgotten a generation following the cholinergic hypothesis, Exp. Neurol. 163 (2000) 495–529.

[13] M. Singh, M. Kaur, H. Kukreja, R. Chugh, O. Silakari, D. Singh, Acetylcholinesterase inhibitors as Alzheimer therapy: From nerve toxins to neuroprotection, Eur. J. Med. Chem. 70 (2013), 165–188.

[14] R. Cacabelos, C. Torrellas, O. Teijido, J.C. Carril, Pharmacogenetic considerations in the treatment of Alzheimer’s disease, Pharmacogenomics 17 (2016) 1041–1074.

[15] M. Noetzli, C.B. Eap, Pharmacodynamic, pharmacokinetic and pharmacogenetic aspects of drugs used in the treatment of Alzheimer’s disease. Clin. Pharmacokinet. 52 (2013), 225–241.

[16] R. Leon, A.G. García, J. Marco-Contelles, Recent advances in the multitarget-directed ligands approach for the treatment of Alzheimer’s disease, Med. Res. Rev. 33 (2013) 139–189.

[17] K.-M. Cho, I.-D. Yoo, W.-G. Kim, 8-Hydroxydihydrochelerythrine and 8-hydroxydihydrosanguinarine with a potent acetylcholinesterase inhibitory activity from Chelidonium majus L., Biol. Pharm. Bull. 29 (2006) 2317-2320.

[18] Y. Lei, L. Liu, X. Tang, D. Yang, X. Yang, F. He, Sanguinarine and chelerythrine: two natural products for mitochondria-imaging with aggregation-induced emission enhancement and pH-sensitive characteristics. RSC

Advances 8 (2018) 3919–3927.

[19] P. Kosina, D. Walterova, J. Ulrichova, V. Lichnovsky, M. Stiborova, H. Rydlova, J. Vicar, V. Krecman, M.J. Brabec, V. Simanek, Sanguinarine and chelerythrine: assessment of safety on pigs in ninety days feeding experiment, Food Chem. Toxicol. 42 (2004) 85–91.

[20] F.-J. Cao, R. Yang, C. Lv, Q. Ma, M. Lei, H.-L. Geng, L. Zhou, Pseudocyanides of sanguinarine and chelerythrine and their series of structurally simple analogues as new anticancer lead compounds: cytotoxic activity, structure-activity relationship and apoptosis induction, Eur. J. Pharm. Sci. 67 (2015) 45–54.

[21] F. Miao, X.J. Yang, Y.N. Ma, F. Zheng, X.P. Song, L. Zhou, Structural modification of sanguinarine and chelerythrine and their in vitro acaricidal activity against *Psoroptes cuniculi*, Chem. Pharm. Bull. 60 (2012) 1508–1513.

[22] X.-J. Yang, F. Miao, Y. Yao, F.-J. Cao, R. Yang, Y.-N. Ma, B.-F. Qin, L. Zhou, In vitro antifungal activity of sanguinarine and chelerythrine derivatives against phytopathogenic fungi, Molecules 17 (2012) 13026–13035.

[23] F. Miao, X.-J. Yang, L. Zhou, H.-J. Hu, F. Zheng, X.-D. Ding, D.-M. Sun, C.-D. Zhou, W. Sun, Structural modification of sanguinarine and chelerythrine and their antibacterial activity, Nat. Prod. Res. 25 (2011) 863–875.

[24] Z. Hou, L.-F. Zhu, X.-C. Yu, M.-Q.Sun, F. Miao, L. Zhou, Design, synthesis, and structure-activity relationship of new 2-aryl-3,4-dihydro-β-carbolin-2-ium salts as antifungal agents, J. Agric. Food Chem. 64 (2016) 2847–2854.

[25] B. Zhou, B. Zhang, X. Li, X. Liu, H. Li, D. Li, Z. Cui, H. Geng, L. Zhou, New 2-aryl-9-methyl-β-carbolinium salts as potential acetylcholinesterase inhibitor agents: synthesis, nioactivity and structure–activity relationship, Sci. Rep. 8 (2018) 1559.

[26] S.D. Phillips, R.N. Castle, A review of the chemistry of the antitumor benzo[c]phenanthridine alkaloids nitidine and fagaronine and of the related anti-tumor alkaloid coralyne, J. Heterocycl. Chem. 18 (1981) 223–232.

[27] L.-F. Zhu, Z. Hou, K. Zhou, Z.-B. Tong, Q. Kuang, H.-L. Geng, L. Zhou, Synthesis, bioactivity and structure-activity relationships of new 2-aryl-8-OR-3,4-dihydroisoquinolin-2-iums salts as potential antifungal agents, Bioorg. Med. Chem. Lett. 26 (2016) 2413–2417.

[28] Y.-N. Ma, X.-J. Yang, L. Pan, Z. Hou, H.-L. Geng, X.-P. Song, L. Zhou, F. Miao, Synthesis of 2-aryl-3,4-dihydroisoquinolin-2-ium bromides and their in vitro acaricidal activity against *Psoroptes cuniculi*, Chem. Pharm. Bull. 61(2013) 204–211.

[29] G.L. Ellman, K.D. Courtney, J.R.V. Andres, R.-M. Featherstone, A new and rapid colorimetric determination of acetylcholinesterase activity, Biochem. Pharmacol. 7 (1961), 88–95.

[30] G. Xiao, Y. Li, X. Qiang, R. Xu, Y. Zheng, Z. Cao, L. Luo, X. Yang, Z. Sang, F. Su, Y. Deng, Design, synthesis and biological evaluation of 4′-aminochalconerivastigmine hybrids as multifunctional agents for the treatment of Alzheimer's disease, Bioorg. Med. Chem. 25 (2017), 1030–1041.

[31] P. Valenti, A. Rampa, A. Bisi, V. Andrisano, V. Cavrini, L. Fin, A. Buriani, P. Giusti, Acetylcholinesterase inhibition by tacrine analogs, Bioorg. Med. Chem. Lett. 7 (1997), 2599–2602.

[32] N. Sultana, M. Sarfraz, S.T. Tanoli, M.S. Akram, A. Sadiq, U. Rashid, M.I. Tariq, Synthesis, crystal structure determination, biological screening and docking studies of N1-substituted derivatives of 2,3-dihydroquinazolin-4(1H)-one as inhibitors of cholinesterases, Bioorg. Chem. 72 (2017), 256–267.

[33] F. Miao, X.-J. Yang, L. Zhou, H.-J. Hu, F. Zheng, X.-D. Ding, D.-M. Sun, C.-D. Zhou, W. Sun. Structural modification of sanguinarine and chelerythrine and their antibacterial activity, Nat. Prod. Res. 25 (2011) 863–875.

Journal Pre-proof

Highlights

- Thirty-one target compounds (**8**) were synthesized.
- Seven compounds possess the potent anti-AChE activity and low cytotoxicity.
- **8y** has the excellent dual AChE−BuChE inhibition activity.
- The compounds bind with AChE by a competitive model and the π-π action.
- The 4′ site is a privileged modifiable position for the high anti-AChE activity.

Journal Pre-proof

Journal Pre-proof

Declaration of interests

☒ The authors declare that they have no known competing financial interests or personal relationships that could have appeared to influence the work reported in this paper.

☐The authors declare the following financial interests/personal relationships which may be considered as potential competing interests:

Journal Pre-proof